Journal of Power Sources 195 (2010) 1647–1656

Contents lists available at ScienceDirect

Journal of Power Sources

journal homepage: www.elsevier.com/locate/jpowsour

Local online gas analysis in PEFC using tracer gas concepts

Gabriel A. Schuler, Alexander Wokaun, Felix N. Büchi*

Electrochemistry Laboratory, Paul Scherrer Institut, CH-5232 Villigen PSI, Switzerland

ARTICLE INFO

Article history:
Received 7 July 2009
Received in revised form
21 September 2009
Accepted 26 September 2009
Available online 7 October 2009

Keywords:
PEFC
Online gas analysis
Local species distribution
Membrane permeation
Water vapor distribution

ABSTRACT

Comprehension of gas phase transport processes and species distribution in operating polymer electrolyte fuel cells (PEFC) is an important task for understanding and optimizing the related coupled processes. Few efforts for in-situ gas analysis in fuel cells are described in the literature, and previous work has focused mainly on integral species concentration or investigation in small laboratory scale cells under comparably dry conditions only. In this work, a methodology for flexible local in-situ gas analysis in polymer electrolyte fuel cells of technical size is presented. This includes conceptual description of measurement modes during fuel cell operation in particular for local membrane and gas diffusion layer characterization. Beside characterization of the analysis system, the potential of the method is demonstrated by accurate local concentration measurement of gas species including water vapor up to saturated conditions. Accurate measurement of local membrane tracer gas permeation under open circuit and load conditions emphazises the flexibility of the developed methodology. In particular, the ability to determine local membrane permeation characteristics is of great value for membrane degradation investigation.

1. Introduction

Mass transport processes in polymer electrolyte fuel cells (PEFC) occur on a wide range of scales driven by different gradients. Most mass transport processes are related to gaseous species and/or transport in the gas phase. Some of the processes, for example reactant transport in the porous materials, are crucial for fuel cell operation and optimization is desired. Others, such as reactant transport through the electrolyte membrane negatively influence efficiency or lifetime and should be eliminated. Therefore detailed generic understanding of local gas phase properties and the related transport processes preferentially under real world operating conditions is required. This understanding requires in-situ investigation of the gas phase and its temporal and local changes with appropriate experimental hardware. Reports on gas phase investigation in PEFC are rare, especially those providing local information, due to the need of significant additional instrumentation.

Gas phase investigations of fuel cells described in the literature can be classified by the type of gas phase access, the size of the investigated cell, the underlying measurement intention and the used sensor or analysis technology. For local species analysis, the gas phase is either contacted in-situ by optical pathways or miniaturized sensors or gas is extracted through small capillaries. The integration of sensors for local species analysis without disturbing fuel cell operation is difficult and has been demonstrated only for local humidity [1,2] measurement. Therefore in the following a more detailed review of only optical and gas extracting analysis systems is given.

1.1. Optical systems

Optical pathways are generally rather bulky and therefore difficult to integrate into PEFC cell designs without compromising other functionalities. Therefore optical methods have been primarily used in small laboratory cells or half cells. Measurement intentions range from detailed reaction investigation on catalysts by Fourier transform infrared spectroscopy (FTIR) [3], tunable diode laser absorption (TDLA) for species detection [4] to gas transport investigation by laser induced fluorescence (LIF) [5] or particle image velocimetry (PIV) [6,7].

1.2. Gas extracting systems

Gas extracting measurement techniques have the general advantages of being compatible with different analysis principles and allow for a more flexible cell design due to less bulky connections to the gas phase. Nevertheless, in realistic applications only low amounts of gas can be extracted without disturbing fuel cell operation, which makes also the use of optical gas extracting measurement principles a difficult task. Classically, the two proven techniques for gas analysis with low sample gas consumption are gas chromatography (GC) and mass spectrometry (MS).

* Corresponding author. Tel.: +41 56 310 24 11; fax: +41 56 310 44 15.
E-mail address: felix.buechi@psi.ch (F.N. Büchi).

0378-7753/$ – see front matter © 2009 Elsevier B.V. All rights reserved.
doi:10.1016/j.jpowsour.2009.09.053

First gas analysis investigations of electrochemical laboratory cells and half cells were made by differential electrochemical mass spectrometry (DEMS) [8–10]. In these systems, a mass spectrometer is used for species detection and the analyzing system is separated from the electrochemical components by gas permeable membrane. Later, direct coupling of a fuel cell with the gas analyzer without a separating membrane was shown by Wasmus et al. with the multipurpose electrochemical mass spectrometer technique (MPEMS) [9]. The same technique was used for online investigation by Wang et al. [11] and was termed real time mass spectrometry. All of these efforts did provide only integral information of the gas phase in the cell and the main focus was on the analysis of non-condensable gaseous species. Mench et al. started to investigate water vapor as well, first by gas chromatography [12] and later by mass spectrometry for the first time with local resolution [13,14]. In this set-up, local resolution was achieved by manual sequential attachment of the gas extraction system to different local gas extraction ports.

In general, gas chromatography has the drawback of high hardware complexity for condensable species measurement and long sampling time, therefore the focus has switched to mass spectrometer systems. One of the most sophisticated mass spectrometer based systems for local gas analysis was developed by Partridge et al. [15]. This system was originally designed for local combustion engine exhaust gas catalyst investigations and adapted to laboratory sized solid oxide and polymer electrolyte fuel cells. The gas extracting part of this system was further developed to a commercial product and is available as SpaciMS from Hiden Analytical. The SpaciMS gas extraction system was designed for local gas analysis in high temperature applications such as solid oxide fuel cells and automotive exhaust gas treatment systems and does not have fully heated gas extraction lines for proper adaption to low temperature applications with condensable gaseous species, as present in PEFC. This is a handicap under higher load and generally humid conditions, which can lead to capillary blockage by condensed water and unstable vacuum chamber (VC) pressure conditions.

Gas extracting systems in combination with mass spectrometric analysis is the most flexible combination for local gas analysis in PEFC. Although GC has the advantage of generally lower detection limits, MS is not susceptible to condensable species and has a considerably higher measurement frequency. Despite the previous demonstrations of MS based gas analysis for local properties, there is still a lack of proper adaptation of the main components of an MS based gas analysis system. In fact, only careful adaptation of fully heated gas extraction lines, mass spectrometer and vacuum system to PEFC conditions allows for accurate and highly flexible analysis of both condensable and non-condensable gas species. In addition, existing systems were connected to laboratory cells with single or dual serpentine flow field [13,15] which seldom reflect the behaviour of cells in real applications. Channel cross section dimensions were often enlarged in comparison to real world systems in order to facilitate gas extraction [13].

Therefore the objective of this paper is to present the concept and method of local and online gas phase analysis for PEFC. The gas analysis hardware, measurement principle and flexibility to investigate components as well as local transport and degradation processes under real world operating conditions is described. The sensitivity and potential of this method is demonstrated by determination of local species distribution and local membrane permeation measurements.

2. Concepts for local online gas analysis

Local in-situ gas phase investigation of PEFC can be divided into characterization of local gas phase composition as function of operating conditions and in-situ characterization of the gas transport properties of different components. Analysis of local species concentration is a straightforward measurement and component characteristics can be determined using a tracer gas concept. The general layout of local gas analysis suitable for both applications is shown in Fig. 1. On both anode and cathode side of the cell, two adjacent channels of the flow field are equipped with local, in channel direction distributed, fully heated gas ports (Ai.j, Ci.j). Depending on the selected measurement mode, gas ports can be used for gas extraction or as tracer gas supply line.

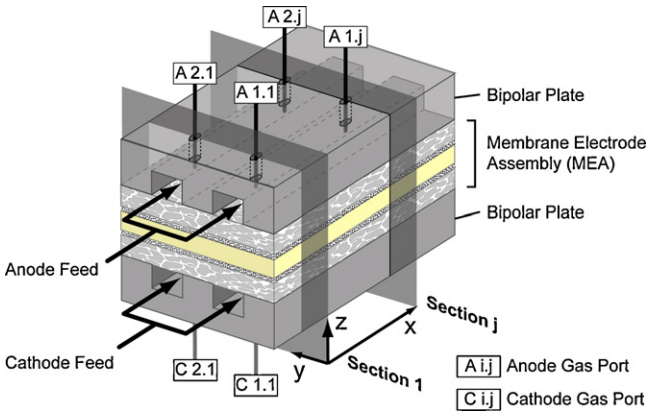

Fig. 1. Cut-out of a PEFC with gas extraction or gas addition ports on anode and cathode sides for local online gas phase investigation.

2.1. Local species concentration along the channel

Due to the flexibility of MS based species detection, local reactant concentration can be measured both on anode and cathode side. Local resolution along the channel is given by the number of gas extraction ports. Few centimeters (typically 2–4 cm) are required as spacing between fully heated gas ports, which allows for sufficient resolution along the channel in cells of technical size. Also water vapor concentration measurement along the channel is possible, as the MS system is not restricted to dry sample gases and gas extraction lines can be fully heated. Still, under condensing conditions the presence of liquid water can interfere with gas extraction by temporarily blocking extraction capillaries.

2.2. Component characterization using tracer gas concepts

In-situ component characterization focuses on permeation behaviour of the membrane electrode assembly (MEA) components. Through-plane membrane permeation and in-plane gas diffusion layer (GDL) permeation characteristics under load conditions, with the respective local liquid water saturations are of high interest. For this task, inert tracer gases are used.

In the case of membrane permeation measurements, an inert tracer is needed because during fuel cell operation an unknown ratio of the permeating reactant species directly reacts on the catalyst of the permeate side and it's determination in the gas channel can therefore not serve as an accurate indicator for the membrane gas separation properties. Gas permeation through the MEA in through-plane direction during fuel cell operation can therefore be measured by addition of tracer gas to the feed gas stream on one side of the MEA and local measurement of permeated tracer gas concentration on the opposite side. Fig. 2A shows the principle of this measurement mode with helium as hydrogen and nitrogen as oxygen tracer. As the membrane is the most dense barrier for through-plane MEA gas transport, this measurement mode is highly useful for investigating local membrane degradation with

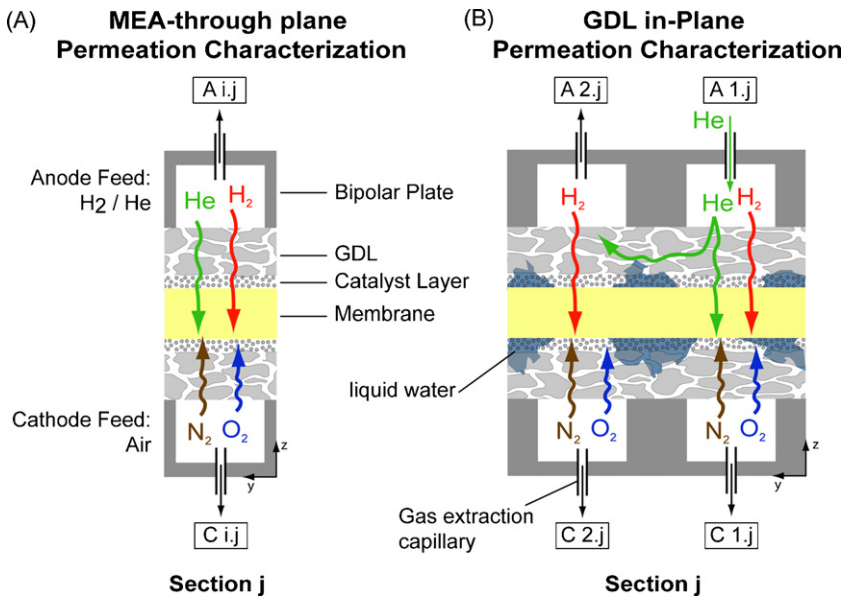

Fig. 2. Concepts for investigating permeation properties using tracer gas. Positions of sections are indicated in Fig. 1. (A) Layout for online through-plane MEA permeation. (B) Layout for online in-plane gas diffusion layer (GDL) characterization.

respect to changes of its local gas separation properties. Comparison of the spatially resolved diffusive permeation (driving force: partial pressure gradient only) and convective permeation (driving forces: absolute and partial pressure gradients) serves as indicator of the local state of health of the membrane with respect to its gas separation properties. The inert tracer gases have different molecule sizes and different solubilities in the membrane material which cause different gas permeation characteristics. Still, if measured continuously during the lifetime of the cell, they can be used as inert tracer for membrane integrity. The stable and low detection limit of helium makes this tracer particularly interesting, in the following all tracer gas experiments are based on helium.

A similar tracer gas concept as for the membrane characterization can be used for studying in-plane GDL diffusion characteristics under various operating conditions. In this case, the tracer gas has to be introduced as a marker in one of the first gas ports of a single channel (Fig. 1, A2.1 or A1.1) and is not added to the general feed gas stream. Subsequent permeation of the tracer gas through the GDL is measured downstream in the neighboring channel (Fig. 2b). Even though this measurement set-up is not demonstrated within this work, it allows for characterization of gas diffusion layers and flow field combinations for various operating conditions and cell geometries.

3. Experimental set-up

3.1. Fuel cell hardware

A fuel cell of technical size with a linear flow field, an active area of 200 cm^2 and channel dimensions of $0.8 \times 0.5 \times 400$ mm has been adapted with gas extraction lines. Bipolar plates are machined from carbon and PVDF based Sigracet BMA5 (SGL Carbon) plates. Electrochemical components used are Nafion N112 membranes and Etek Elat (A6 STDSI V2.1) carbon cloth gas diffusion layer (GDL) with catalyst loading of 0.5 mg cm^{-2}. Outside the active area, the membrane is reinforced by Mylar foils (DuPont) of 12 μm thickness. Cell compression is adjusted by teflon spacers to uniform compress the GDL to 70% of its initial thickness. The cell can be operated in counterflow (hydrogen and air fed from opposite sides) or co-flow (both gases fed from the same side).

3.2. Gas analysis hardware

On anode and cathode side, 11 gas extraction ports for local gas analysis are distributed equally along the length of the channel in the middle of the active cell area (see Fig. 3). Two additional gas extraction ports are placed at the in- and outlet of the cell to measure integral gas compositions. Gas is extracted out of the flow field channel by polyimide coated fused silica capillaries with a diameter of 50 microns (SGE 0624635). The extracted gas flows to a subsequent selector valve (VICI, EMT3CSD16UWE, RSV in Fig. 4). These valves allow for the sequential selection of local gas ports on anode and cathode side. Polyimide coated fused silica capillaries (SGE 062472) of 150 μm diameter are used to connect the selector valves to the vacuum chamber (VC) of the mass spectrometer. Connections between capillaries and bipolar plate are sealed with gas chromatography septa (CHROMSEAL 9001-LL) to ensure gas tight connection with minimum sealing force applied. Sealing of the capillaries at the valve fittings is provided by polyimide ferrules (VICI FS1.2–5). Each gas extraction line is permanently heated by custom made thermally insulated heating capillaries.

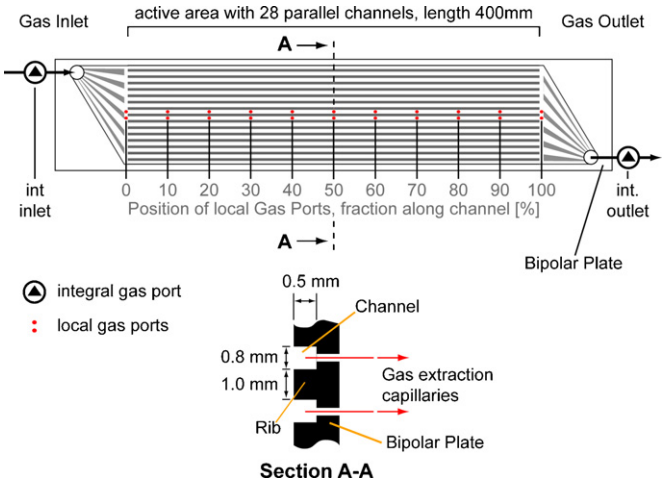

Fig. 3. Linear flow field with gas extraction ports and detail of channel dimensions including gas extraction capillaries.

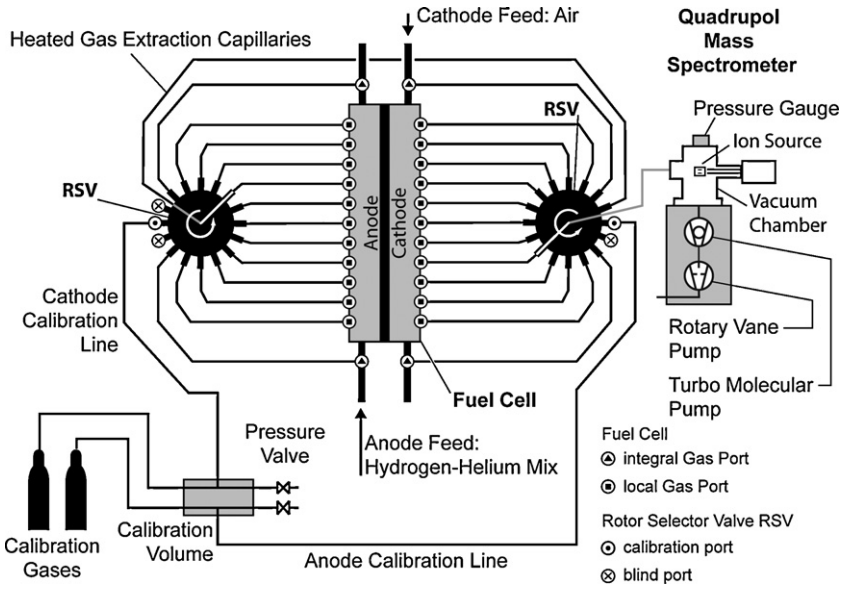

Fig. 4. Layout of local online gas analysis by mass spectrometry.

Temperature of these capillaries is set to 120 °C and controlled by temperature sensors (Pt100) in conjunction with a multi channel temperature controller (ELOTECH R2500). Both selector valves are placed in thermally insulated boxes and heated to 130 °C. This fully heated gas extraction line provides non-condensing, constant and stable sample gas extraction and ensures constant pressure levels in the vacuum chamber. The bipolar plate under the gas port shows no temperature increase due to the heating of the capillaries. The custom made vacuum chamber is made from stainless steel 316L. Thermal annealing at 950 °C for 1 h under vacuum conditions (5E-5-1E-4 mbar) and subsequent cool down under nitrogen atmosphere reduced the material hydrogen content and therefore the hydrogen measurement background.

Conventional copper sealing was used for all vacuum proof connections of the VC. The VC is permanently heated to 90 °C to avoid the build up of background signals due to condensing gas species. The total pressure in the VC is measured by a combined pirani and cold cathode gauge (Pfeiffer PKR261). Capillary dimensions were adjusted to lead to total pressure levels in the VC between 1e-6 and 1e-5 mbar during valve switching and fuel cell operating pressure levels between 1 and 2.5 bar(abs). Extracted gas is ionized in the VC by an open cross beam ion source with tungsten filaments (Pfeiffer). Ionized gas species are analyzed in the subsequent quadrupole mass spectrometer (Pfeiffer Prisma 200M1, length 200 mm, rod diameter 6 mm). The built-in channeltron is used as ion detector. Vacuum conditions in the VC are maintained by a turbo molecular pump (Pfeiffer TSU261) in conjunction with a rotary vane prepump (Pfeiffer DUO 5M). High vacuum pumping power of this pump combination ensures fast and sufficient VC conditioning at valve switching between local gas ports and test rig start up.

3.3. Calibration hardware

Retaining identical species ionization probabilities and ion current amplification in the mass spectrometer during the entire measurement period is crucial. Therefore, calibration routines were run at the beginning of new experiments and in regular time intervals. The good calibration stability of the mass spectrometer allowed for extending calibration intervals to one week under continuous operation. They consist of quadrupole offset adjustment, secondary electron multiplier (SEM) voltage adjustment and gas specific calibration. Mass spectrometer calibration at fuel cell pressure levels is provided by the independent and fully heated calibration volume (Fig. 4). Certified calibration gas mixtures (Messer) were used to determine gas calibration factors. During all calibration routines and measurements, constant ion source cathode voltage of 80 V, ion source emission current of 0.7 mA, MS resolution of 50 and a sampling time per mass between 0.5 and 2 s was used.

4. Characterization of the gas analysis system

The sensitivity and accuracy of gas phase investigation in PEFC depends on various factors such as signal quality and fuel cell operating conditions, therefore sample gas consumption, signal to noise behaviour, MS sensitivity and measurement dynamics of the system have been characterized.

4.1. Sample gas consumption

With the given capillary combination a maximum of 37 μl min^{-1} gas is extracted out of a single flow field channel. This volume of extracted gas accounts for less than 0.5% of the stoichiometric excess gas of a single channel under a current density of 1 A cm^{-2} and a stoichiometry of 1.5 on anode or cathode side, respectively. Even under limited feed gas operation at a stoichiometry of 1.1 and current density of 0.1 A cm^{-2}, the extracted gas accounts for less than 9% of the stoichiometric excess gas in a single channel. Therefore cell disturbance due to the extracted sample gas is considered negligible.

4.2. Quality and sensitivity

To test the sensitivity of the set-up, analogue mass spectrometry scans in the mass range 1–45 were conducted on selector valve (Fig. 4, RSV) blind ports and measurement ports to analyze the signal to noise ratio. Fig. 5 shows the results for the cathode side. Comparably high background ion current during the blind port scan on the masses 28 and 32 indicate small air leaks in the gas extraction line. Leakage of this size would not be acceptable in analytical MS systems. However, with restrictive peak analysis this drawback is tolerable because on the cathode side only nitrogen, oxygen, water and helium are analyzed. Measurement to background ion current

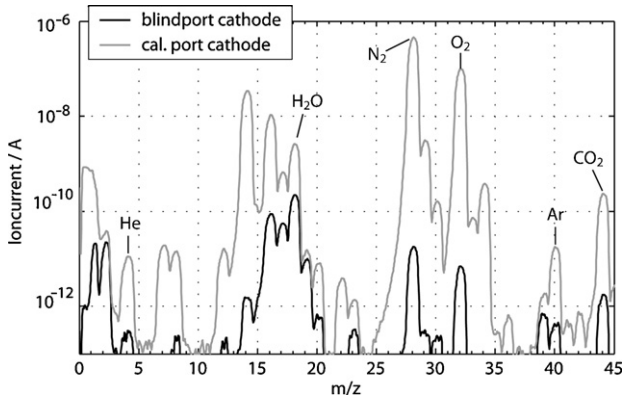

Fig. 5. Signal (grey) to noise (background scan, black) conditions of the gas extraction line in blind port and fuel cell gas extraction operation on the cathode side. Focus on helium and restrictive peak evaluation allows for accurate measurements despite the air leakage of the gas extraction line.

ratios of these species are at least one order of magnitude and therefore sufficient for the purpose. On the anode side the focus is on the detection of hydrogen and helium, as the signal to background ratio of permeated nitrogen from the cathode is low and makes this measurement critical.

The quality of the gas extraction system in conjunction with MS may be characterized by species sensitivities (E_i) and minimum detectable concentrations based on MS-noise level (c_{md}), blind port background level (c_{bg}) and combined fuel cell mass flow controller and pressure controller induced concentration fluctuation (c_{op}). The detection limits were measured with the calibration line in order to separate fuel cell test bench influence from real cell operation fluctuations. Table 1 shows the data for hydrogen and helium at the anode and in Table 2 for nitrogen, oxygen and helium at the cathode. The sensitivities of the species decrease in the order $N_2 > O_2 > H_2 > He$ and reflect the well known nitrogen referenced ionization probabilities within the ion source.

Tables 1 and 2 show that operating induced fluctuations from the fuel cell test bench are more limiting than MS analysis inherent errors for all gas species, except for helium detection at the cathode side. In the case of helium measurement at the cathode side, operating induced errors are below the background concentration detection limit of 2.5 ppm. In the running system however, background levels of extraction lines are limiting, because the drawback of operating induced errors can be suppressed by longer sampling times and better statistics. Therefore, minimum detectable species concentrations are in the range of 2.5–61 ppm on anode and cathode sides. These detection limits are sufficient for most measurement applications. In most detection limit critical measurement cases, species concentration levels can be shifted to lower dilution on the permeate side to mitigate detection limits problems (e.g. by lower stoichiometry).

Table 3
Vacuum chamber pressure fluctuation induced calibration error on the anode side at 1.5 bar(abs) fuel cell pressure.

Anode species	Calibration gas concentration (mol mol^{-1})	Relative error (−)
H_2	9.49E-01	1.1E-04
He	5.14E-02	2.0E-03

Table 4
Vacuum chamber pressure fluctuation induced calibration error on the cathode side at 1.5 bar(abs) fuel cell pressure.

Cathode species	Calibration gas concentration (mol mol^{-1})	Relative error (−)
N_2	7.95E-01	6.0E-04
O_2	2.05E-01	2.0E-03
He	1.00E-04	3.5E-02

4.3. Calibration quality

Inevitable port to port VC pressure differences under measurement conditions occur due to capillary assembly inequalities, valve port machining tolerances and fuel cell pressure gradients along the channel. Mass spectrometer calibration factors represent the linear relationship between species concentration and measured ion current at a given VC pressure level. Because of the VC pressure dependence of calibration factors, calibration volume pressure scans in the range of port to port VC pressure fluctuations were conducted. Tables 3 and 4 show the relative calibration errors due to VC pressure fluctuations of local gas analysis on anode and cathode sides at 1.5 bar fuel cell pressure. Considering the complexity of the gas extraction line, these relative error levels are considered fairly good and sufficient for afore mentioned fuel cell investigation concepts.

Calibration of water vapor concentration in gas mixtures of GC or MS systems is generally a difficult task which needs highly sophisticated and very constant humidifying systems. Karlegärd et al.

Table 1
Anode species sensitivity.

Anode species	Calibration gas concentration (mol mol^{-1})	Sensitivity E (A mbar^{-1})	c_{md}[a] (mol mol^{-1})	c_{bg}[b] (mol mol^{-1})	c_{op}[c] (mol mol^{-1})
H_2	9.49E-01	1.3E-01	4.9E-07	6.1E-05	2.2E-02
He	5.1 4E-02	5.0E-02	2.0E-07	1.2E-06	1.2E-03

[a] Mass spectrometer based detection limit.
[b] Vacuum chamber background induced detection limit.
[c] Fuel cell test bench induced detection limit.

Table 2
Cathode species sensitivity.

Cathode species	Calibration gas concentration (mol mol^{-1})	Sensitivity E (A mbar^{-1})	c_{md}[a] (mol mol^{-1})	c_{bg}[b] (mol mol^{-1})	c_{op}[c] (mol mol^{-1})
N_2	7.95E-01	3.4E-01	3.2E-05	1.3E-05	2.0E-02
O_2	2.05E-01	2.9E-01	3.8E-07	1.3E-05	6.0E-03
He	1.00E-04	6.7E-02	1.7E-06	2.5E-06	1.5E-06

[a] Mass spectrometer based detection limit.
[b] Vacuum chamber background induced detection limit.
[c] Fuel cell test bench induced detection limit.

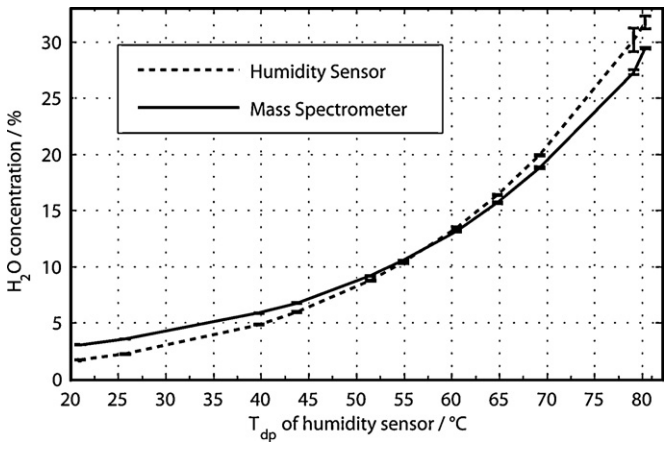

Fig. 6. Comparison of water vapor concentration measurements in air with mass spectrometer (MS) and humidity sensor (HS, Vaisala HMP247) at 1.5 bar (abs) pressure.

[16] avoided this difficulty in an online analysis system for gasification gas by utilizing the fact of identical ionization probabilities of nitrogen and water vapor. A combined comparative reference measurement with a capacitive humidity sensor (Vaisala HMP247) and the mass spectrometer was conducted in order to check the applicability of this calibration routine. Fig. 6 shows this comparison with a maximum difference of 2.5% between MS and humidity sensor measurement. Above dew points of 40 °C, this difference lies within the accuracy range of the humidity sensor. In the dew point range below 40 °C, MS based measurement shows a maximum error of 1.5%, what is more than the humidity sensor error in this dew point range. MS measurement has the advantage of more stable signals even at high humidity levels. More precise MS based water vapor measurement could be made by multipoint calibration in conjunction with precise and stable humidity generators. Considering the achieved accuracy and signal stability, this easy calibration scheme is sufficient and accurate enough for local fuel cell water vapor analysis.

4.4. Dynamics of the gas analysis system

The dynamics of the gas analysis system defines the time for species concentration measurements along the sampling channel of the fuel cell. The dynamics is given by the times for valve switching, capillary flushing, VC conditioning and sampling time on the gas port. Anode side helium addition experiments were conducted in order to demonstrate the gas analysis dynamics with species of low molecular weight at two different concentration levels. Fig. 7 shows the helium concentration at the first anode gas port of the flow field (10% range) and integral outlet gas port at the cathode side (500 ppm range) during a 10% helium addition to the anode feed gas stream. Helium addition was started at $t = 0$ and stopped at the time indicated in the figure. These plots show stable measurement conditions 20 s after the start of helium addition. This includes roughly 10 s for capillary flushing and mass flow controller delay time. A similar capillary flushing time in the order of 10 s and a VC helium conditioning time of about 20 s are visible after the stop of the helium addition. Fast helium concentration decay on both, anode and cathode side show good VC conditioning in different concentration ranges. VC conditioning of condensable water vapor is the second relevant factor for measurement dynamics. Dew point step measurements from 79 to 27 °C showed that sufficient conditioning of 10 °C in dew point is possible within 10 s. Water vapor conditioning in this range is sufficient for measurement along the fuel cell channel. These conditioning times of non-condensable and condensable species in the different concentration ranges illustrate the importance of proper MS and vacuum system adaptation.

Afore mentioned system dynamics allow a full concentration profile along a fuel cell channel including eleven local and two integral gas ports with a sampling time of 5 s per gas ports in less than 6 min. Fast fuel cell changes can be measured by continuous single gas port sampling, taking into account the capillary flushing delay of approximately 10 s.

5. Results and discussion

Besides the above outlined system characterization, the gas analysis method needs to prove its high sensitivity under fuel cell relevant conditions. To demonstrate the potential of this technique, permeation and species measurement under open circuit (OCV) and load conditions are presented and discussed in this section.

5.1. Permeation measurements under open circuit conditions

Under OCV conditions mass and volume flow in the anode and cathode are constant along the channel as no relevant sinks and sources for educts and products are present, except for the very small amount of permeating species. Local helium permeate concentration measurements under OCV conditions along the cathode channel are shown in Fig. 8. For these measurements, 10% helium was added to the anode feed as tracer gas. The cell was operated at different temperatures with a constant relative humidity of the feed

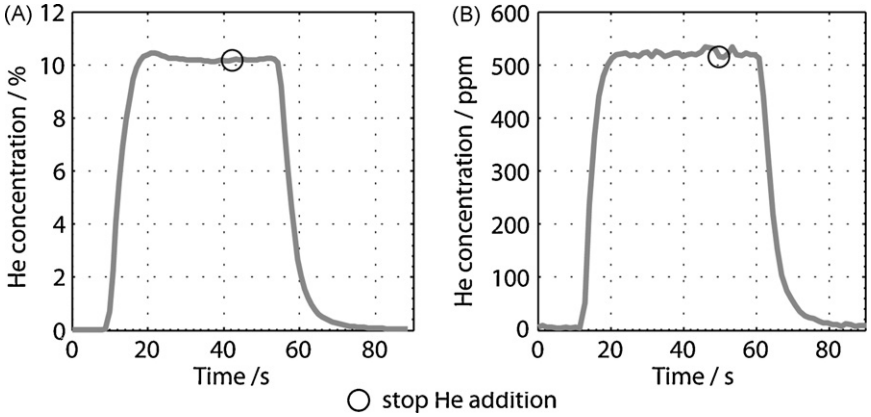

Fig. 7. Measurement of gas extraction line dynamics and vacuum chamber conditioning with 10% helium addition on the anode side. (A) Helium measurement at the first anode side gas port; (B) helium measurement at the integral outlet gas port on the cathode. Flow regime: Counterflow; $p_a = p_c = 1.5$ bar (abs), $T_{capillary} = 120$ °C.

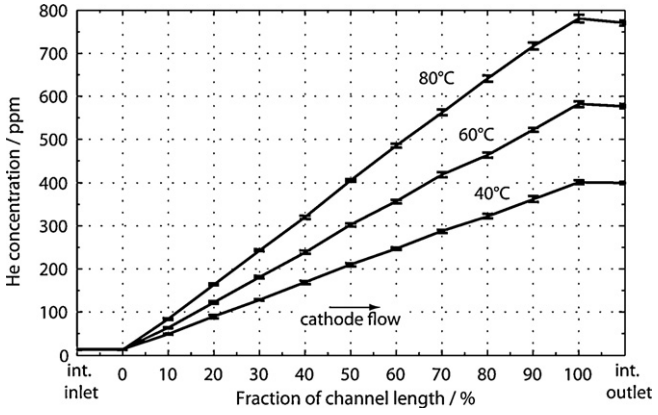

Fig. 8. Local helium permeate concentration at cathode under open circuit conditions. T_{cell} = 40 °C, 60 °C, 80 °C; $p_a = p_c$ = 1.5 bar(abs); Anode: 90% H_2, 10% He, V = 0.5 l_n min^{-1}, rH = 46%; Cathode: 100% air, V = 0.5 l_n min^{-1}, rH = 50%; counterflow.

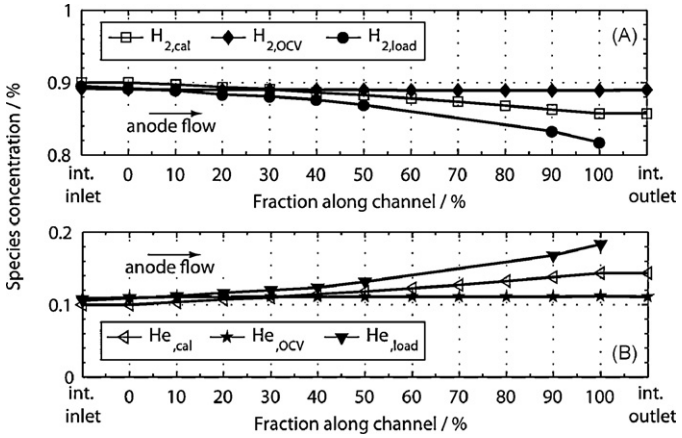

Fig. 9. Calculated (cal) and measured species concentration on anode side at OCV and at 0.375 A cm^{-2}. T_{cell} = 80 °C; $p_a = p_c$ = 1.5 bar (abs); Anode: 90% H_2, 10% He, λ = 3, rH = 46%; Cathode: 100% air, λ = 2, rH = 50%, Counterflow. (A) Hydrogen; (B) Helium.

gases of 50% on cathode and 46% on the anode side and flow rates at anode and cathode of 0.5 l min^{-1} dry gas at 1.5 bar(abs). Linear helium permeate concentration increases along the channel with low signal scattering are observed. The linear increase of helium concentration at the cathode indicates that local helium permeability is constant over the entire active area of the cell and can easily be evaluated from the slope of the helium increase. Helium permeability rises from $2.4 \pm 0.1 * 10^{(-14)}$ (mol m^{-1} s^{-1} Pa^{-1}) at 40 °C to $5 \pm 0.1 * 10^{(-14)}$ (mol m^{-1} s^{-1} Pa^{-1}) at 80 °C which corresponds to a permeability increase of 6.5e-16 (l K^{-1}). Considering differences in experimental approaches and hardware used for ex-situ measurements, these values compare well to literature data [17,18,19] and show the high sensitivity and accuracy of the in-situ methodology. Under OCV conditions, the evaluation of the permeation is straightforward and accurate because of the constant mass flows at the permeate (cathode) and feed side (anode). At the integral inlet gas port the helium background of air (5 ppm, see Fig. 8) is observed and the equal concentrations at the integral outlet gas port and the last local port in the active area show that under non-condensing OCV conditions, the sensed channel is representative for all parallel channels of the flow field.

The sensitivity of local permeation measurements under OCV conditions could further be tuned by adaptation of the tracer gas concentration on the feed side and the dilution level on the permeate side. This would allow to increase permeate concentration levels already at the first gas port in the active area in order to enhance the local permeability sensitivity. However, generally one aims for minimal tracer gas addition on the feed side in order to induce least influence to the fuel cell operation. Tuning is limited because the MS calibration is concentration dependent, and maximum species concentrations variation should lie within approximately two decades of the calibration concentration to keep calibration errors below 10% relative. The measurement in Fig. 8 shows that sufficient resolution is already obtained at the second gas port within the active area under the given dilution conditions. Based on the ratio of maximum concentration (770 ppm) in comparison to the calibration concentration (100 ppm), there is still room for enhancement of the resolution by a factor of about 13. This tuning is limited by the minimum stable flow conditions on the permeate side, which is given by the accuracy and stability of the mass flow and pressure controllers of the fuel cell test bench. For the case shown in Fig. 8 tracer gas addition and permeate side dilution reduction by a factor of 5 could further increase measurement accuracy. The results in Fig. 8 and afore outlined tuning possibilities illustrate the high tracer gas sensitivity of MS based local gas analysis under OCV conditions.

5.2. Local species measurements under load conditions

For local gas analysis, load conditions at relevant humidity levels pose considerably higher difficulties than OCV conditions due to the possible presence of condensing conditions in parts of the cell. The chosen operating conditions of hydrogen/helium (90%/10%) at the anode and air at the cathode at 1.5 bar(abs) with relative gas humidities of 50% at cathode and 46% at anode result in high humidity and condensation at the cathode as well as at the anode. Figs. 9 and 10 show measured and calculated local species concentrations at anode and cathode side under OCV and load conditions of 75 A (0.375 A cm^{-2}) after 5 min set point conditioning. Species concentrations are given as molar fractions of dry gases. The measurement error bars, of less than 1% absolute are not shown for better marker visibility. Reactant gas consumption and relative inert gas increase along the channels are clearly visible under load conditions for both the anode and cathode.

Clear differences between calculated and measured concentrations are visible at anode and cathode towards the respective gas outlets. This indicates that the sensed channel is different from the average having a higher than average stoichiometric consumption of the respective reactant. The reason for this behaviour can be higher than average local current density over the sampling channel and/or unequal feed gas distribution to the channels of the flow field due to condensation effects, which are not considered in the calculated values. Detailed differentiation between these two cases

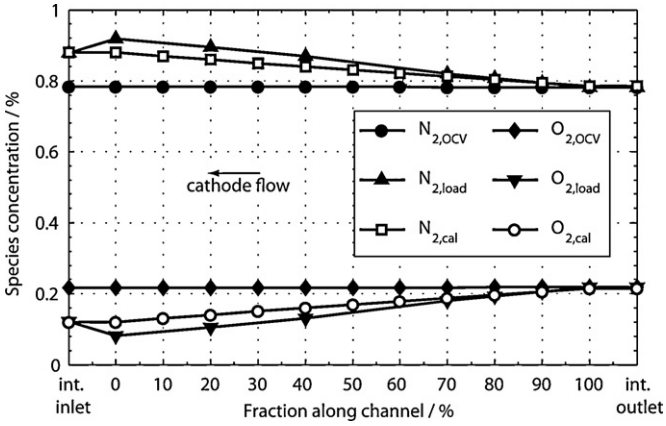

Fig. 10. Calculated (cal) and measured species concentration on cathode side at OCV and at 0.375 A cm^{-2}. T_{cell} = 80 °C; $p_a = p_c$ = 1.5 bar(abs); Anode: 90% H_2, 10% He, λ = 3, rH = 46%; Cathode: 100% air, λ = 2, rH = 50%, Counterflow.

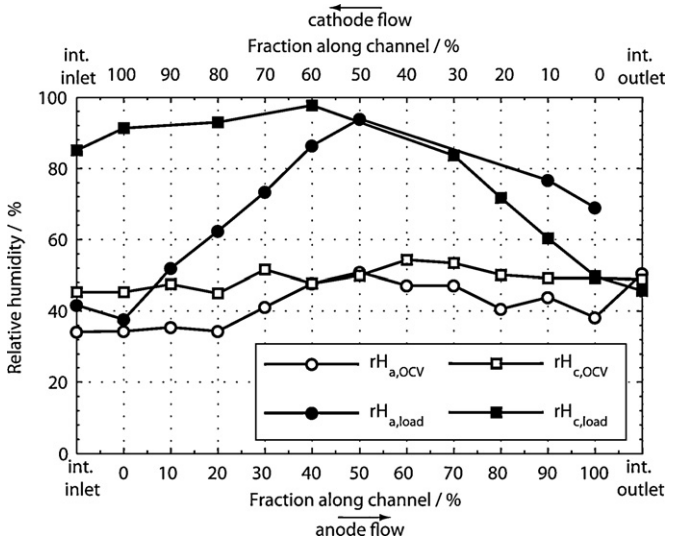

Fig. 11. Local water vapor distribution on anode and cathode side at OCV and at 0.375 A cm^{-2}. T_{cell} = 80 °C; $p_a = p_c$ = 1.5 bar(abs); Anode: 90% H_2, 10% He, λ = 1.5, rH = 46%; Cathode: 100% air, λ = 2, rH = 50%; counterflow.

is difficult without additional quantitative species flux information in the sampling channel. These effects of local current density differences and/or non-uniform gas distribution are averaged at the integral outlet gas ports and the calculated and measured values match well. The deviation visible i.e. on the cathode side between calculated and measured values is real and shows the high accuracy of the MS based measurement.

For the same operating conditions, measured water vapor is shown in Fig. 11 as relative local humidity along the channel at cathode and anode for OCV and the load condition at 0.375 A cm^{-2}. Humidity levels under OCV conditions show some noise, which is assumed to stem from water accumulation in the gas diffusion layer and the load history of the cell before the OCV measurement. The data recorded at 0.375 A cm^{-2} in Fig. 11 indicates that saturated conditions at the cathode are visible between 40% and 60% of the channel length. Calculations predict that cathode side exit relative humidity would reach 99% under the given operating conditions and the assumptions of non-condensing conditions within the gas diffusion media and the absence of water transport to the anode. Comparing this to the results in Fig. 11 indicates condensing conditions in the middle part of the cathode channel. This can only be explained by water transport characteristics of the membrane in counterflow operated cells. The water transport to the anode side in the second half of the cathode channel and subsequent water back diffusion from anode to cathode in the first half of the cathode channel enable saturated conditions in the middle of the cathode channel under the given operating condition. Water vapor saturation at the anode is visible at about 60% of the channel length. Subsequent dry out of the anode towards the outlet stems from water drag and low cathode side humidity, which is typical for cells operated in counterflow mode. Freunberger et al. [20] investigated water management phenomena with a 1 + 1D model and showed similar membrane water transport trends.

Conditions of more than 80% local relative humidity tend to increase the risk of gas port blockage due to condensed water at the capillary tip. Blocked capillaries are temporarily not usable for gas analysis as can be seen from missing points at few positions under load conditions in Figs. 9–11. Depending on the amount of condensed water within the channel and gas diffusion media, capillaries can be deblocked autonomously or by increased stoichiometry. Despite temporary capillary blockage, the trends of relative humidity along the channel are measureable with reasonably low scattering and allow interpretation of the present local humidification state within the cell.

5.3. Permeation measurements under load condition

Similarly as shown in Fig. 8 for OCV conditions, the membrane permeation can be measured under load conditions. Again the local permeation measurement is based on helium permeation. Helium is added as tracer gas to the anode feed gas stream and permeates to the cathode side. However, in comparison to OCV measurements, interpretation of permeation data under load is more complicated due to the following facts: (i) hydrogen consumption at the anode increases the local helium concentration and thus the driving force for the diffusive helium transport through the membrane along the channel; (ii) similarly, permeated tracer gas is diluted in variable volumes of gas along the cathode channel due to oxygen consumption. As a consequence, constant MEA permeation characteristics will result in different measured concentration profiles along the channel depending on the gas stoichiometries. Hence, local MEA permeation measurement under load requires local species analysis on anode and cathode side. Measured helium permeation data on the cathode has to be corrected according to the local helium concentration along the anode channel as well as oxygen depletion and permeate accumulation along the cathode channel. Additional influences under load conditions may be induced due to the non-uniformities observed in the local species concentration measurements, i.e. current density deviations under the sample channel and/or non-uniformities of the feed gas distribution to the parallel channels due to water accumulation.

Fig. 12 shows calculated anode helium concentration increase due to hydrogen consumption along the channel with an initial gas mixture of 90% hydrogen and 10% helium. For stoichiometries higher than 2 an almost linear behaviour of the local helium concentration is observed. However a significant exponential increase towards the cell outlet occurs for stoichiometries of 1.5 and less. This is of importance, as anode stoichiometries in this range are relevant in technical applications. Analogue profiles can be plotted for the cathode side. Due to the use of air as feed gas on the cathode, the exponential behaviour is significantly smaller because here the reactant is the minority species. In addition, the situation at the cathode is less critical because the permeated helium can be referenced to the constant nitrogen gas flux.

In Fig. 13, measured accumulative helium permeate concentration on the cathode side under OCV and load conditions are shown. Concentration measurement of permeated helium traces at the cathode are possible with small fuel cell operation induced errors

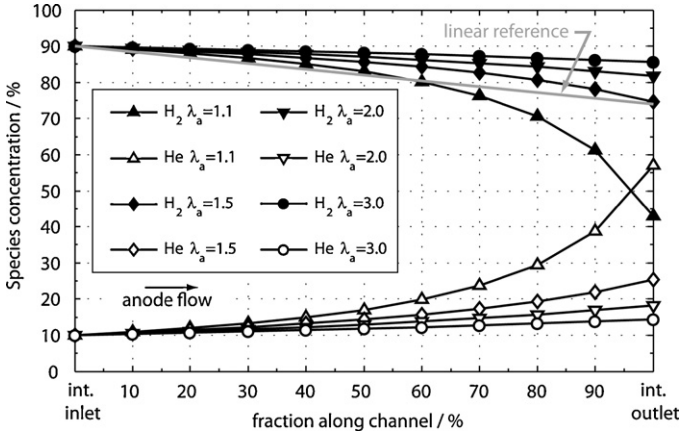

Fig. 12. Calculated relative concentration profiles of local anode gas composition as function of the stoichiometry. Anode inlet mixture: 90% H_2, 10% He.

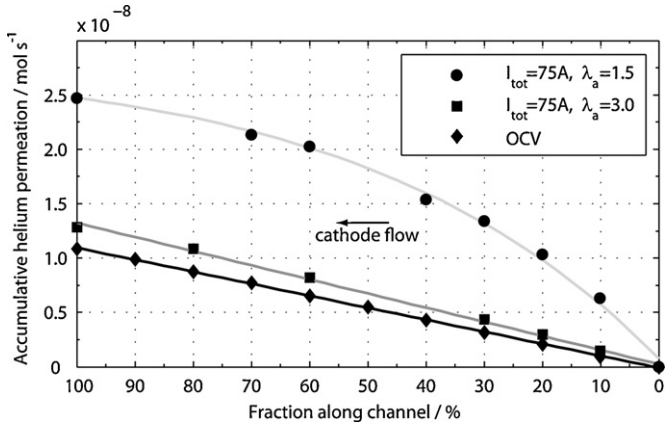

Fig. 13. Helium permeate concentration on cathode side at OCV and under load conditions of 0.375 A cm^{-2} (75 A); at anode stoichiometries of $\lambda(H_2)$ = 1.5 and 3.0; T_{cell} = 80 °C; $p_a = p_c$ = 1.5 bar(abs); Anode: 90% H_2, 10% He, rH = 46%; Cathode: 100% air, λ = 2, rH = 50%; counterflow.

of less than 1.5% relative, because constant and stable gas extraction conditions and the resulting constant pressure in the vacuum chamber allow stable ionization conditions in the MS. The important influence of the anode feed gas supply is illustrated by the difference between the measurements with hydrogen stoichiometries of 1.5 and 3.0. In this measurement, again the slope of the accumulated helium concentration on the cathode represents the local helium permeation. Under high anode stoichiometry and OCV conditions, the slope is constant and evaluation of the local helium permeation is easy.

For calculating effective membrane gas transport characteristics under load conditions at low anode stoichiometries, local helium permeation has to be corrected by the local diffusive driving force, the partial helium pressure difference over the membrane (i.e. helium concentration at the anode). However under load at low anode stoichiometry the different uncertainties of local permeability calculation cumulate. Varying helium partial pressure along the anode channel and/or uneven current and gas distribution in the flow field contribute most to the total local permeability calculation uncertainty. Additionally, low stoichiometry and condensing conditions in the anode channel reduce the number of usable anode gas ports in the second half of the channel. The resulting calculated local helium permeability is plotted in Fig. 14. The error bars indicate the large error of local helium permeability calculation in the second half of the channel in the 1.5 stoichiometry case. While for the

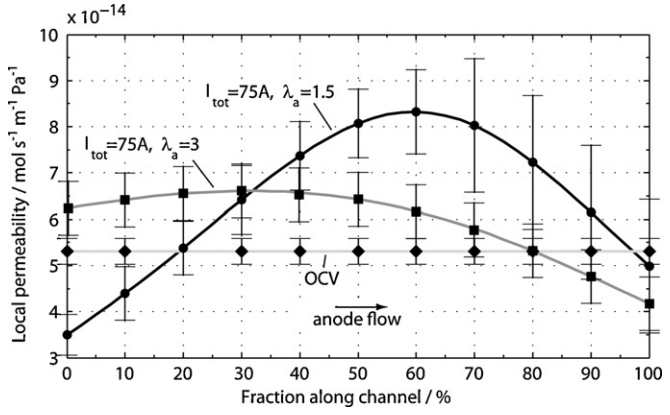

Fig. 14. Local helium permeability calculated from local permeation measurement under OCV and load condition at 0.375 A/cm^2 (75 A) with different anode stoichiometries in counterflow operation. $p_a = p_c$ = 1.5 bar(abs); T_{cell} = 80 °C; Anode: 90% H_2, 10% He, rH = 46%; Cathode: 100% air, λ = 2, rH = 50%.

OCV condition an accurate membrane permeation characteristic is obtained with an error of 6%, the data for the permeation measurements under load shows a considerable noise. Hence, online permeate concentration measurement using helium as tracer gas is possible with high accuracy (see Fig. 13), but determination of local membrane permeability has a significantly lower accuracy, with an error between 20% and 75% due to the uncertainties of the local anode helium partial pressure distribution.

In conclusion, the application of MS based gas analysis in PEFC under load conditions has a high accuracy for local reactant concentration even under realistic humidity conditions, membrane permeation using helium as tracer gas is measured most accurately under OCV conditions.

6. Conclusion

Understanding the gas phase transport processes and species distribution in PEFC requires appropriate methodology for local gas phase analysis. Carefully adapted mass spectrometry components in conjunction with fully heated and sequentially selectable gas extraction lines have been designed for local gas analysis in PEFC under fuel cell relevant operating conditions. Measurements up to fully saturated water vapor conditions are possible. This local online gas analysis methodology is therefore a flexible tool with competitive dynamics for different tasks ranging from simple species distribution measurements along the channel to more complex membrane permeation and diffusion media characterization under open circuit and load conditions. Based on a tracer gas concept using helium, online membrane permeation is measured very accurately under OCV conditions. Under load current conditions tracer gas concentration measurement is also possible with high accuracy. However, determination of effective membrane permeation under load is less accurate due to tracer concentration variation at the feed gas side, in particular when low stoichiometries at the feed gas side are used. Nevertheless, the possibility to accurately measure species concentration along the channel in PEFC allows for various future investigations and better understanding of gas transport processes in PEFC.

Acknowledgements

We would like to thank Thomas Gloor and Marcel Hottiger for their support concerning test bench build up and hardware maintenance. We gratefully acknowledge financial support for the mass spectrometer gas analysis system development from the Swiss Federal Office of Energy (SFOE) under grant 101785.

References

[1] G. Hinds, M. Stevens, J. Wilkinson, M. de Podesta, S. Bell, J. Power Sources 186 (2009) 52–57.
[2] H. Nishikawa, R. Kurihara, S. Sukemori, T. Sugawara, H. Kobayasi, S. Abe, T. Aoki, Y. Ogami, A. Matsunaga, J. Power Sources 155 (2006) 213–218.
[3] I. Tkach, A. Panchenko, T. Kaz, V. Gogel, K.A. Friedrich, E. Roduner, Phys. Chem. Chem. Phys. 6 (2004) 5419–5426.
[4] S. Basu, H. Xu, M.W. Renfro, B.M. Cetegen, J. Fuel Cell Sci. Technol. 3 (2006) 1–7.
[5] F. Barreras, A. Lozano, L. Valiño, C. Marín, A. Pascau, J. Power Sources 144 (2005) 54–66.
[6] L. Grega, M. McGarry, M. Begum, B. Abruzzo, J. Fuel Cell Sci. Technol. 4 (2007) 272–279.
[7] S.Y. Yoon, J.W. Ross, M.M. Mench, K.V. Sharp, J. Power Sources 160 (2006) 1017–1025.
[8] B. Bittins-Cattaneo, S. Wasmus, B. Lopez-Mishima, W. Vielstich, J. Appl. Electrochem. 23 (1993) 625–630.
[9] S. Wasmus, S.R. Samms, R.F. Savinell, J. Electrochem. Soc. 142 (1995) 1183–1189.
[10] S.E. Smith, E. Casado-Rivera, H.D. Abruna, J. Solid State Electrochem. 7 (2003) 582–587.
[11] J. Wang, S. Wasmus, R.F. Savinell, J. Electrochem. Soc. 143 (1996) 1233–1239.
[12] M.M. Mench, Q.L. Dong, C.Y. Wang, J. Power Sources 124 (2003) 90–98.

[13] Q. Dong, J. Kull, M.M. Mench, J. Power Sources 139 (2005) 106–114.
[14] Q. Dong, M.M. Mench, S. Cleghorn, U. Beuscher, J. Electrochem. Soc. 152 (2005) A2114–A2122.
[15] W.P. Partridge, T.J. Toops, J.B. Green, T.R. Armstrong, J. Power Sources 160 (2006) 454–461.
[16] A. Karlegärd, A. Götz, I. Bjerle, Chem. Eng. Technol. 18 (2004) 183–192.
[17] J.S. Chiou, D.R. Paul, Ind. Eng. Chem. Res. 27 (1988) 2161–2164.
[18] T. Sakai, H. Takenaka, N. Wakabayashi, Y. Kawami, E. Torikai, J. Electrochem. Soc. 132 (1985) 1328–1332.
[19] S.S. Kocha, J.D. Yang, J.S. Yi, AIChE J. 52 (2006) 1916–1925.
[20] S.A. Freunberger, M. Santis, I.A. Schneider, A. Wokaun, F.N. Büchi, J. Electrochem. Soc. 153 (2006) A396–A405.